$$H_2 = 6G_{222}d_2A_2 + (G_{212}/2)(A_1^2 - B_1^2)$$
$$H_3 = 0$$
$$H_4 = \tfrac{3}{2}G_{222}(A_2^2 - B_2^2)$$
$$\bar{H}_0 = 0$$
$$\bar{H}_1 = 0$$
$$\bar{H}_2 = 6G_{222}d_2B_2 + G_{212}A_1B_1$$
$$\bar{H}_3 = 0$$
$$\bar{H}_4 = 3G_{222}A_2B_2$$
$$C = G_{121}[(2d_2A_1 + A_1A_2 + B_1B_2)\cos\omega\tau + (A_1A_2 - B_1B_2)\cos 3\omega\tau + (2d_2B_1 - B_1A_2 + A_1B_2)\sin\omega\tau + (A_1B_2 + B_1A_2)\sin 3\omega\tau]$$

References

[1] Eisley, J. G. and Bennett, J. A., "Stability of Large Amplitude Forced Motion of a Simply Supported Beam," *International Journal of Nonlinear Mechanics*, Vol. 5, Dec. 1970, pp. 645–657.

[2] Bennett, J. A. and Eisley, J. G., "A Multiple Degree-of-Freedom Approach to Nonlinear Beam Vibrations," *AIAA Journal*, Vol. 8, No. 4, April 1970, pp. 734–739.

[3] Efstathiades, G. J. and Williams, C. J. H., "Vibration Isolation Using Non-Linear Springs," *International Journal of Mechanical Sciences*, Vol. 9, No. 1, Jan. 1967, pp. 27–44.

[4] Min, G. B. and Eisley, J. G., "Nonlinear Vibration of Buckled Beams," *Journal of Engineering for Industry*, Vol. 94, No. 2, May 1972, pp. 1137–1146.

[5] Tseng, W.-Y. and Dugundji, J., "Nonlinear Vibrations of a Beam Under Harmonic Excitation," *Journal of Applied Mechanics*, Vol. 37, No. 2, June 1970, pp. 292–297.

[6] Tseng, W.-Y. and Dugundji, J., "Nonlinear Vibrations of a Buckled Beam Under Harmonic Excitation," *Journal of Applied Mechanics*, Vol. 38, No. 2, June 1971, pp. 467–476.

[7] Hayashi, C., *Nonlinear Oscillations in Physical Systems*, McGraw-Hill, New York, 1964, pp. 28–30.

[8] Grove, W. E., *Brief Numerical Methods*, Prentice-Hall, Englewood Cliffs, N.J., 1966, pp. 19–24.

MAY 1973 AIAA JOURNAL VOL. 11, NO. 5

Nonlinear Finite Element Analysis of Sandwich Shells of Revolution

PARVIZ SHARIFI*
Lockheed Missiles & Space Company Inc., Sunnyvale, Calif.

AND

E. P. POPOV†
University of California, Berkeley, Calif.

The nonlinear bending and buckling problems of axisymmetric three-layered sandwich shells are solved using an incremental finite element approach. The nonlinearities considered are due to large displacements, and plastic deformations of the facings. The sandwich construction is assumed to have identical facings and isotropic material properties. Flexural, extensional, and shear stiffnesses of all three layers are considered. The discrete model is obtained using a doubly curved axisymmetric shell element. An incremental variational principle is employed to derive the element equilibrium equations. These equations contain a load correction term which gives better accuracy and convergence. To illustrate the applicability of the method to nonlinear bending and buckling problems, three examples are solved. The finite element solutions compare favorably with the available analytical and experimental results.

Introduction

RECENTLY, the finite element discretization technique has been applied to linear and nonlinear analysis of sandwich structures.[1–3] Abel and Popov[1] applied the method to a linear analysis of axisymmetric shells including the in-plane and bending effects of the core as well as those of the facings. Also, Monforton and Schmit, using a totally different discrete model, solved the linear[2] and large displacement[3] problems of soft core sandwich plates and cylinders.

Received March 31, 1972; presented as Paper 72-356 at the AIAA/ASME/SAE 13th Structures, Structural Dynamics, and Materials Conference, San Antonio, Texas, April 10–12, 1972; revision received December 15, 1972.

Index categories: Structural Static Analysis; Structural Stability Analysis.

* Research Specialist. Member AIAA.

† Professor of Civil Engineering. Associate Fellow AIAA.

Herein, an incremental displacement formulation for the nonlinear finite element analysis of sandwich shells of revolution with axisymmetrical loadings and boundary conditions is presented. The nonlinearities considered are due to large displacements as a result of finite rotations, and plastic deformations of facings. The incremental variational principle, including a "load correction" term, is used to derive the element equilibrium equations. In this derivation, a moving reference configuration is considered; and in the plastic range, von Mises yield criterion together with isotropic hardening rule are used.

The discrete model is obtained using a doubly curved axisymmetrical shell element. The element has a three-layered sandwich construction with similar facings. Homogeneous and isotropic material properties are assumed; and flexural, extensional, and shear deformations of all three layers are considered. With this formulation, monocoque shells can be analyzed by simply assigning the same material properties to all of the sandwich layers. However, this is not applicable in the plastic

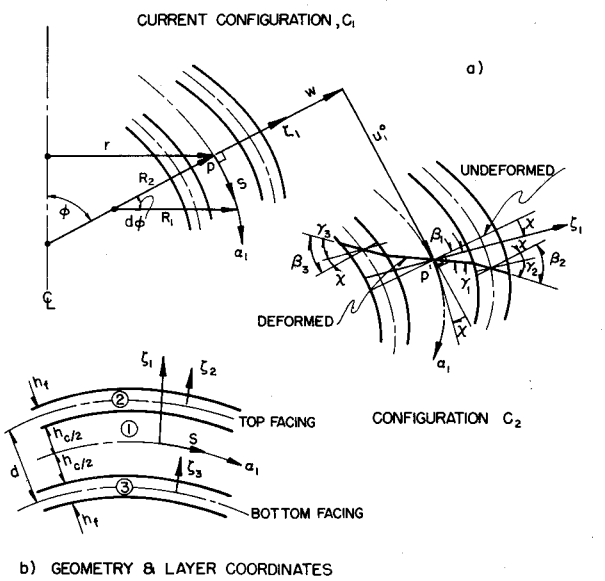

Fig. 1 Kinematics of incremental axisymmetric deformation of a sandwich shell.

range where the plastic deformation of the core layer is neglected in the present formulation.

The method is applied to investigate the nonlinear bending and buckling behavior of axisymmetric plates and shells of monocoque as well as sandwich construction. For postbuckling analysis, the finite element equations are augmented to give a positive-definite stiffness matrix in the descending branch of the load-deflection curve. To show the capability and accuracy of the method, the results are compared with some of the analytical and experimental results available in the literature.

Kinematics of the Incremental Deformation

The meridional profile of the sandwich shell under consideration is shown in Fig. 1. Here h_c and h_f designate the thicknesses of the core and facings, respectively. The surface curvilinear coordinates are denoted by α_1 and α_2 (not shown) which coincide with the lines of principal curvatures in the meridional and hoop directions, respectively. Also ζ_1, ζ_2, and ζ_3 designate the normal coordinates of the core, top, and bottom facings with their origins at the respective middle surfaces (see Fig. 1b). Henceforth, the subscripts 1, 2, and 3 are assigned to the quantities associated with the core, top, and bottom facings, respectively.

Figure 1a shows the incremental deformation characteristics of the shell between the current configuration, C_1, and a neighboring one, C_2. The quantities ${u_1}^0$, and w are, respectively, the incremental meridional and transverse displacements of a generic point P located on the middle surface of the shell in C_1. As shown, the deformed cross sections do not remain normal to the tangent to the middle surface of the shell. Denoting the rotations of the cross section of the layers by β_k and that of the tangent to the middle surface by χ, the following relation holds:

$$\beta_k = \chi + \gamma_k, \quad k = 1,2,3 \tag{1}$$

in which γ_1, γ_2, and γ_3 are the incremental shear strains in the core, top, and bottom facings, respectively. As the two facings are assumed to be identical, $\gamma_2 = \gamma_3$ and $\beta_2 = \beta_3$. Following Abel,[1] γ_k are assumed to be constant in each layer. This results in a discontinuity of shear deformations in the interfaces. The difference is accounted for by the warpage of the cross section γ defined as

$$\gamma = \gamma_c - \gamma_f \tag{2}$$

where $\gamma_c = \gamma_1$ and $\gamma_f = \gamma_2 = \gamma_3$.

Neglecting the normal deformations in the thickness direction, the incremental displacement field can be written as

$$u_k(\alpha_1, \zeta_k) = {u_k}^0(\alpha_1) + \zeta_k \beta_k(\alpha_1) \tag{3a-c}$$

$$w_k(\alpha_1, \zeta_k) = w(\alpha_1), \quad k = 1,2,3 \tag{3d-f}$$

Here ${u_1}^0$, ${u_2}^0$, and ${u_3}^0$ denote the meridional displacements of the middle surfaces of the core, top and bottom facings, respectively. By imposing the continuity of the meridional displacements at the interfaces, it can be shown that

$${u_2}^0(\alpha_1) = {u_1}^0(\alpha_1) + \tfrac{1}{2}[h_c \beta_1(\alpha_1) + h_f \beta_2(\alpha_1)] \tag{4a}$$

$${u_3}^0(\alpha_1) = {u_1}^0(\alpha_1) - \tfrac{1}{2}[h_c \beta_1(\alpha_1) + h_f \beta_3(\alpha_1)] \tag{4b}$$

Following Novozhilov,[16] the nonlinear incremental strain-displacement relations including the effects of transverse shear deformations of an axisymmetric monocoque shell are derived in Appendix A. Introducing Eqs. (1) and (3) into Eqs. (A3, A4, and A6) of Appendix A, the incremental strain-displacement relations in each layer of the sandwich shell are obtained. In this derivation the continuity of the linear and nonlinear components of the extensional strains at the interfaces of the layers is maintained. The resulting relations can be written as

$$(\varepsilon_{11})_k = (e_{11})_k + (\eta_{11})_k \tag{5a}$$

$$(\varepsilon_{22})_k = (e_{22})_k + (\eta_{22})_k, \quad k = 1,2,3 \tag{5b}$$

$$(2\varepsilon_{13})_k = (2e_{13})_k + (2\eta_{13})_k \tag{5c}$$

where ε_{11} and ε_{22} are, respectively, the extensional strains in the meridional and hoop direction, and ε_{13} is the transverse shear strain. In Eqs. (5) for each kth layer

$$(e_{11})_k = ({e_{11}}^0)_k + \zeta_k ({\kappa_{11}}^1)_k \tag{6a}$$

$$(e_{22})_k = ({e_{22}}^0)_k + \zeta_k ({\kappa_{22}}^1)_k \tag{6b}$$

$$(2e_{13})_k = (2{e_{13}}^0)_k \tag{6c}$$

are the linear components, and

$$(\eta_{11})_k = ({\eta_{11}}^0)_k + \zeta_k ({\kappa_{11}}^2)_k \tag{7a}$$

$$(\eta_{22})_k = ({\eta_{22}}^0)_k + \zeta_k ({\kappa_{22}}^2)_k \tag{7b}$$

$$(2\eta_{13})_k = (2{\eta_{13}}^0)_k \tag{7c}$$

are the nonlinear components of the incremental strain tensor. In Eqs. (6), for $k = 1$

$${e_{11}}^0 = e_{1c} \tag{8a}$$

$${e_{22}}^0 = e_{2c} \tag{8b}$$

$$2{e_{13}}^0 = \gamma_c \tag{8c}$$

and for $k = 2, 3$

$${e_{11}}^0 = e_{1c} \pm (d/2)(\kappa_{1x} + r_c \kappa_{1c} + r_f \kappa_{1f}) \tag{8d}$$

$${e_{22}}^0 = e_{2c} \pm (d/2)(\kappa_{2x} + r_c \kappa_{2c} + r_f \kappa_{2f}) \tag{8e}$$

$$2{e_{13}}^0 = \gamma_f \tag{8f}$$

are the linear components of incremental strains in the middle surfaces of core and facings, respectively, and

$${\kappa_{11}}^1 = \kappa_{1x} + \kappa_{1c} \tag{9a}$$

$${\kappa_{22}}^1 = \kappa_{2x} + \kappa_{2c} \quad \text{for} \quad k = 1 \tag{9b}$$

and

$${\kappa_{11}}^1 = \kappa_{1x} + \kappa_{1f} \tag{9c}$$

$${\kappa_{22}}^1 = \kappa_{2x} + \kappa_{2f} \quad \text{for} \quad k = 2,3 \tag{9d}$$

are the linear components of incremental curvature changes in core and facings, respectively. In Eqs. (7), for $k = 1$

$${\eta_{11}}^0 = \tfrac{1}{2}({e_{1c}}^2 + \chi^2) \tag{10a}$$

$${\eta_{22}}^0 = \tfrac{1}{2}(e_{2c})^2 \tag{10b}$$

$$2{\eta_{13}}^0 = (\chi + \gamma_c) e_{1c} \tag{10c}$$

and for $k = 2, 3$

$${\eta_{11}}^0 = \tfrac{1}{2}({e_{1c}}^2 + \chi^2) \pm (d/2)(\kappa_{1x} + r_c \kappa_{1c} + r_f \kappa_{1f}) e_{1c} \pm (d/4R_1)(\chi^2 - r_c {\gamma_c}^2 - r_f {\gamma_f}^2) \tag{10d}$$

$${\eta_{22}}^0 = \tfrac{1}{2}{e_{2c}}^2 \pm (d/2)(\kappa_{2x} + r_c \kappa_{2c} + r_f \kappa_{2f}) e_{2c} \mp (d/4r)[r_c(\chi + \gamma_c)^2 + r_f(\chi + \gamma_f)^2] \sin\phi \tag{10e}$$

$$2{\eta_{13}}^0 = (\chi + \gamma_f) e_{1c} \tag{10f}$$

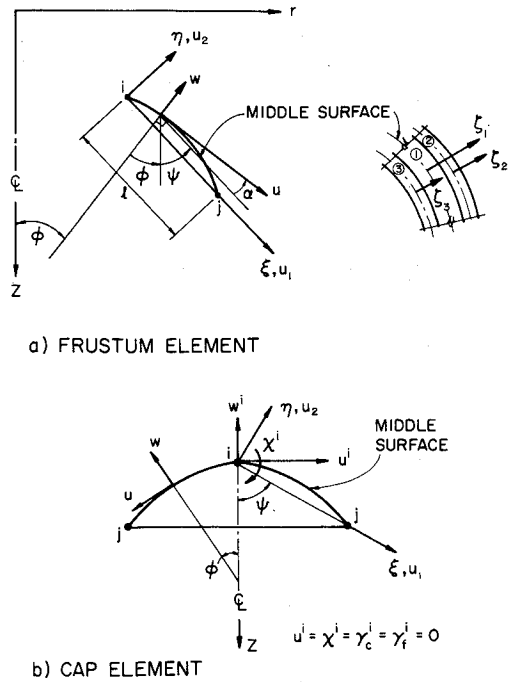

Fig. 2 Doubly curved shell element.

are the nonlinear components of incremental strains in the middle surfaces of core and facings, respectively, and for $k = 1$,

$$\kappa_{11}{}^2 = (\kappa_{1x}+\kappa_{1c})e_{1c}+(1/2R_1)(\chi^2-\gamma_c{}^2) \tag{11a}$$

$$\kappa_{22}{}^2 = (\kappa_{2x}+\kappa_{2c})e_{2c}-(1/2r)(\chi+\gamma_c)^2\sin\phi \tag{11b}$$

and for $k = 2,3$

$$\kappa_{11}{}^2 = (\kappa_{1x}+\kappa_{1f})e_{1c}+(1/2R_1)(\chi^2-\gamma_f{}^2) \tag{11c}$$

$$\kappa_{22}{}^2 = (\kappa_{2x}+\kappa_{2f})e_{2c}-(1/2r)(\chi+\gamma_f)^2\sin\phi \tag{11d}$$

are the nonlinear components of the incremental curvature changes in core and facings, respectively. The quantities appearing in Eqs. (8–11) are defined as

$$e_{1c} = du_1{}^0/ds+w/R_1;\quad e_{2c} = (1/r)(u_1{}^0\cos\phi+w\sin\phi)$$

$$\kappa_{1x} = d\chi/ds;\quad \kappa_{2x} = (\chi/r)\cos\phi;\quad \chi = u_1{}^0/R_1-dw/ds$$

$$\kappa_{1c} = d\gamma_c/ds;\quad \kappa_{2c} = (\gamma_c/r)\cos\phi;\quad \kappa_{1f} = d\gamma_f/ds;$$

$$\kappa_{2f} = (\gamma_f/r)\cos\phi$$

$$r_c = h_c/d;\quad r_f = h_f/d;\quad r = R_2\sin\phi;\quad ds = R_1\,d\phi$$

where R_1 and R_2 are the principal radii of curvature, s is the arc length, and ϕ is the coordinate angle in the meridional direction (see Fig. 1). The sign convention for the increments of displacements and rotations are shown in Fig. 1.

Incremental Constitutive Relations

Consistent with the formulation of the problem under consideration, the constitutive equations are written for an incremental step between configurations C_1 and C_2. In view of the application of these equations in the subsequent derivation of equilibrium equations, it is imperative to use the Piola symmetric stress tensor, s_{ij}, as the measure of incremental stresses. This stress is defined in terms of the unit area and the coordinates of the reference configuration, C_1. Furthermore, the derivation is subject to the following assumptions: 1) deformations (strains) are infinitesimal, but rotations are finite; 2) the core material is elastic; 3) in the inelastic range for the facings, a) the plastic flow is governed by von Mises yield criterion and isotropic hardening rule, and b) shear stresses have negligible effect on the plastic behavior of the facings.

In Appendix B an incremental elastic-plastic constitutive relation for a three-dimensional homogeneous body is derived using Cartesian tensors. Introducing the appropriate physical components of the stresses, strains, and metric tensors of the shell surface coordinates into Eqs. (B11) and (B12) of Appendix B, the required constitutive relations are obtained.[4] For the case of generalized plane-stress, the result can be written as

$$\begin{Bmatrix} s_{11} \\ s_{22} \\ s_{13} \end{Bmatrix}_k = \begin{bmatrix} C_{11} & C_{12} & 0 \\ C_{21} & C_{22} & 0 \\ 0 & 0 & C_{13} \end{bmatrix}_k \begin{Bmatrix} \varepsilon_{11} \\ \varepsilon_{22} \\ 2\varepsilon_{13} \end{Bmatrix}_k, \quad k = 1,2,3 \tag{12}$$

where

$$(C_{11})_k = \left\{\frac{A^3}{B}\frac{E}{\Omega}[\rho+(1-\rho)S_2{}^2]\right\}_k;\quad (C_{13})_k = \left\{\alpha\frac{A}{B}G\right\}_k$$

$$(C_{22})_k = \left\{\frac{B^3}{A}\frac{E}{\Omega}[\rho+(1-\rho)S_1{}^2]\right\}_k$$

and

$$(C_{12})_k = (C_{21})_k = \left\{AB\frac{E}{\Omega}[\nu\rho-(1-\rho)S_2S_1]\right\}_k$$

In these equations, for each layer (designation k is deleted): α = shear correction factor; $\rho = E_t/E$; $\Omega = (1-\nu^2)\rho+(1-\rho)\times(S_1{}^2+2\nu S_1S_2+S_2{}^2)$; $A = (1+2{}^1\varepsilon_{11})^{1/2}$; $B = (1+2{}^1\varepsilon_{22})^{1/2}$; $S_1 = (A/B)[({}^1\tau_{11}-\frac{1}{2}{}^1\tau_{22})/\bar{\sigma}]$; $S_2 = (B/A)[({}^1\tau_{22}-\frac{1}{2}{}^1\tau_{11})/\bar{\sigma}]$; and $\bar{\sigma} = ({}^1\tau_{11}{}^2-{}^1\tau_{11}{}^1\tau_{22}+{}^1\tau_{22}{}^2)^{1/2}$ where E and E_t are Young's and tangent moduli, respectively, G is the shear modulus, ν is the Poisson's ratio, ${}^1\tau_{\alpha\beta}$ and ${}^1\varepsilon_{\alpha\beta}$ are, respectively, Cauchy stress and Lagrangian strain tensors in C_1, and $\bar{\sigma}$ is the so-called effective stress. Note that by specifying $\rho = 1$, the stress-strain relations in Eq. (12) degenerate into the corresponding elastic constitutive relations. In the subsequent derivations, consistent with the assumption (2), ρ is set equal to 1 for the core layer ($k = 1$).

Finite Element Formulation

Element Characteristics

For discretizing the shell geometry, a doubly curved axisymmetric ring element is used. This was first developed by Khojasteh-Bakht,[5] and was later modified in Ref. 6. The meridional profile and the local coordinates, (ξ,η), of the element under consideration are shown in Fig. 2. Note that the abcissa is divided by the cord length, l, resulting in $0 \leqq \xi \leqq 1$. The cap element, shown in Fig. 2b, is used for the top of the closed shells; and the frustum elements, shown in Fig. 2a, are used elsewhere. At the end nodal points, i and j, the positions and slopes of the middle surfaces of these elements match with those of a given shell. Thus, the shape of the middle surface of an element, in meridional direction, is given by

$$\eta = \xi(1-\xi)(a_1+a_2\xi) \tag{13}$$

where $a_1 = \tan\alpha_i$, $a_2 = -(\tan\alpha_i+\tan\alpha_j)$, and the angle α is defined in Fig. 2a.

Element Displacement Pattern

In terms of element local coordinates, the following displacement model is assumed for a frustum element, Fig. 2a

$$\begin{aligned} u_1 &= \alpha_1+\alpha_2\xi+\alpha_3\xi^2+\alpha_4\xi^3 \\ u_2 &= \alpha_5+\alpha_6\xi+\alpha_7\xi^2+\alpha_8\xi^3 \\ \gamma_c &= \alpha_9+\alpha_{10}\xi+\alpha_{11}\xi^2 \\ \gamma_f &= \alpha_{12}+\alpha_{13}\xi+\alpha_{14}\xi^2 \end{aligned} \tag{14a–d}$$

where u_1 and u_2 are components of incremental displacements of the middle surface of the element in the directions of ξ and η, respectively; γ_c and γ_f are the incremental shear strains in core and facings, respectively; α_1 and $\alpha_2,\ldots,\alpha_{14}$ are the generalized coordinates. As shown in Fig. 3, ten degrees of freedom at the nodes i and j are the external *DOF*: and four *DOF* at the internal nodes m, n, and k are the internal *DOF*. At each node, i and j, the external *DOF* consist of two displacements u_1 and u_2, one rotation χ, and two shear strains

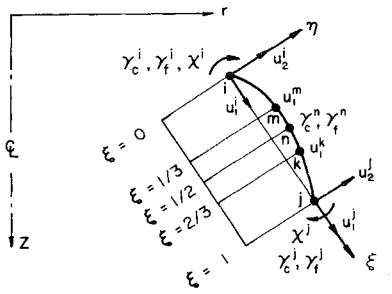

Fig. 3 Internal and external DOF.

γ_c and γ_f. The internal *DOF* consist of two displacements $u^m{}_1$ and $u^k{}_1$, respectively, at nodes m and k, and two shear strains $\gamma_c{}^n$ and $\gamma_f{}^n$ at node n. The locations of the internal nodes are shown in Fig. 3. The following relations hold between the new variables (u_1, u_2) and the displacement components (u, w)

$$u = u_1 \cos\alpha + u_2 \sin\alpha$$
$$w = -u_1 \sin\alpha + u_2 \cos\alpha \qquad (15a\text{–}b)$$

Because of axisymmetric deformation, the displacement component u, the shearing deformations γ_f and γ_c, and the rotation χ must vanish at the top node of the cap element, Fig. 2b. By imposing these conditions, the displacement model in Eq. (14) is specialized for the cap element,[4] and is given by

$$u_1 = -\alpha_3 \cos\Psi + \alpha_4\xi + \alpha_5\xi^2 + \alpha_6\xi^3$$
$$u_2 = \alpha_3 \sin\Psi + \alpha_4 \tan\alpha_i\,\xi + \alpha_7\xi^2 + \alpha_8\xi^3 \qquad (16a\text{–}d)$$
$$\gamma_c = \alpha_{10}\xi + \alpha_{11}\xi^2, \quad \gamma_f = \alpha_{13}\xi + \alpha_{14}\xi^2$$

For subsequent use the matrix representation of the displacement models, Eqs. (14) and (16), can be recast as

$$\{u(\xi)\} = [\phi(\xi)]\{\alpha\} \qquad (17)$$

where

$$\{u(\xi)\}^T = \langle u_1(\xi) u_2(\xi) \chi(\xi) \gamma_c(\xi) \gamma_f(\xi) \rangle$$
$$\{\alpha\}^T = \langle \alpha_1, \alpha_2, \ldots, \alpha_{14} \rangle$$

and

$$[\phi(\xi)]^T = [\phi_{u1}\phi_{u2}\phi_x\phi_c\phi_f]$$

are the displacement functions which except for ϕ_x are given in Eqs. (14) and (16), and ϕ_x is obtained by using Eq. (15) to express χ in the following form:

$$\chi = (\cos^2\alpha/l)[(du_1/d\xi)\tan\alpha - du_2/d\xi]$$

Equilibrium Equations

The element equilibrium conditions can be stated in the variational form of an incremental expression of virtual work. This expression is derived by obtaining the difference between the virtual work expressions of the deformed bodies in configurations C_1 and C_2, written with reference to current configuration C_1. On this basis, the required variational equation has been originally derived in Ref. 7, and has been later modified to include a load correction term for better accuracy and convergence.[4,8] Neglecting the contribution of the body forces, the linearized form of this expression is given by

$$R_c + \int_a \delta\{u\}^T\{t\}\,da = \int_v \delta\{\eta\}^T\{{}^1\tau\}\,dv + \int_v \delta\{e\}^T\{s\}\,dv \qquad (18)$$

where δ is a variational operator, and R_c is the correction or residual loading term given by

$$R_c = \int_a \delta\{u\}^T\{{}^1t\}\,da - \int_v \delta\{e\}^T\{{}^1\tau\}\,dv \qquad (19)$$

In applying Eq. (18) to derive the element equilibrium equations, the quantities appearing in Eqs. (18) and (19) are defined as follows:

$$\{u\}^T = \langle u_1 u_2 \chi \gamma_c \gamma_f \rangle, \quad \{e\}^T = \langle \{e\}_1{}^T \{e\}_2{}^T \{e\}_3{}^T \rangle$$
$$\{\eta\}^T = \langle \{\eta\}_1{}^T \{\eta\}_2{}^T \{\eta\}_3{}^T \rangle$$

where according to Eqs. (6) and (7) $\{e\}_k{}^T = \langle e_{11} e_{22} 2e_{13} \rangle_k$, and

$$\{\eta\}_k{}^T = \langle \eta_{11} \eta_{22} 2\eta_{13} \rangle_k, \quad k = 1,2,3$$
$$\{s\}^T = \langle \{s\}_1{}^T \{s\}_2{}^T \{s\}_3{}^T \rangle, \quad \{{}^1\tau\}^T = \langle \{{}^1\tau\}_1{}^T \{{}^1\tau\}_2{}^T \{{}^1\tau\}_3{}^T \rangle$$

where

$$\{s\}_k{}^T = \langle s_{11} s_{22} s_{13} \rangle_k$$

are components of the incremental Piola stress tensor, and

$$\{{}^1\tau\}_k{}^T = \langle {}^1\tau_{11}\ {}^1\tau_{22}\ {}^1\tau_{13} \rangle_k, \quad k = 1,2,3$$

are components of the Cauchy stress tensor as defined previously. Furthermore, $\{t\}$ denotes the increments of surface tractions measured per unit area a, $\{{}^1t\}$ denotes the vector of surface tractions in C_1 measured per unit area a, and a and v stand for the boundary area and volume of an element in current configuration, respectively.

Utilizing the element displacement model in Eq. (17) together with the kinematical and constitutive equations (5–12), the expression (18) is integrated numerically to yield

$$\delta\{\alpha\}^T\{Q\} = \delta\{\alpha\}^T[k_o + k_g]\{\alpha\} \qquad (20)$$

where

$$\delta\{\alpha\}^T\{Q\} = \int_a \delta\{u\}^T\{{}^1t + t\}\,da - \int_v \delta\{e\}^T\{{}^1\tau\}\,dv$$
$$\delta\{\alpha\}^T[k_o]\{\alpha\} = \int_v \delta\{e\}^T\{s\}\,dv$$
$$\delta\{\alpha\}^T[k_g]\{\alpha\} = \int_v \delta\{\eta\}^T\{{}^1\tau\}\,dv$$

Since $\delta\{\alpha\}$ are arbitrary variational quantities, they can be deleted from both sides of Eq. (20) to give

$$\underset{14\times1}{\{Q\}} = \underset{14\times14}{[k_o + k_g]}\ \underset{14\times1}{\{\alpha\}} \qquad (21)$$

which is the element equilibrium equation in terms of generalized coordinates. Here, $\{Q\}$ is the load vector, $[k_o]$ and $[k_g]$ are, respectively, the ordinary and geometric stiffness matrices. Prior to assemblage, relations such as Eq. (21) should be expressed in terms of some global coordinates according to the following transformation rule

$$\underset{14\times1}{\{\alpha\}} = \underset{14\times14}{[T]}\ \underset{14\times1}{\{\mathbf{r}\}} \qquad (22)$$

where $[T]$ is a linear transformation matrix, and $\{\mathbf{r}\}$ is the element nodal degrees of freedom in terms of global coordinates. For example, in terms of spherical surface coordinates, $\{\mathbf{r}\}$ can be written as

$$\{\mathbf{r}\}^T = \langle u^i w^i \chi_b{}^i \gamma^i \quad u^j w^j \chi_b{}^j \gamma^j \quad \gamma_f{}^i \gamma_f{}^j u_1{}^m u_1{}^k \gamma_c{}^n \gamma_f{}^n \rangle \qquad (23)$$

and matrix $[T]$ follows from relations (15) and (17). In Eq. (23), $\chi_b = \chi + (\gamma_c h_c + \gamma_f h_f)/d$ is the rotation of the tangent to the middle surface due to bending.[1]

By imposing the continuity of u, w, γ, and χ_b at the interelement boundaries, the element force-displacement relations in global coordinates are assembled to obtain the structural equilibrium equations

$$[K]\{r\} = \{R\} \qquad (24)$$

where $[K]$ and $\{R\}$ are the structural stiffness matrix and load vector, respectively. After imposing the boundary conditions, Eqs. (24) are solved for the incremental displacements $\{r\}$. Then using the preceding kinematical and constitutive relations, the incremental strains and stresses are calculated and the solution continues with the next load increment.

Postbuckling Analysis

Perhaps the most significant application of the present nonlinear analysis is for the solution of the buckling problems. For such problems, it is often of practical value to determine the postbuckling behavior of the system. Unlike flat plates, the buckling of shells coincides with a sudden failure accompanied by a large decrease in the load carrying capacity. From an analytical point of view, this means that the descending branch of the load-deflection curve, in the postbuckling region, is characterized by an indefinite stiffness matrix. Therefore, to be able to apply Eqs. (24) in these situations, a special numerical technique must be adopted. Here the method used is based on the idea of augmenting the structure so that the resulting stiffness matrix becomes positive-definite in the postbuckling region. This technique was used in Ref. 9 to solve the buckling problem of frames. Recently, it has been generalized to apply to any structure under arbitrary loading.[4,8]

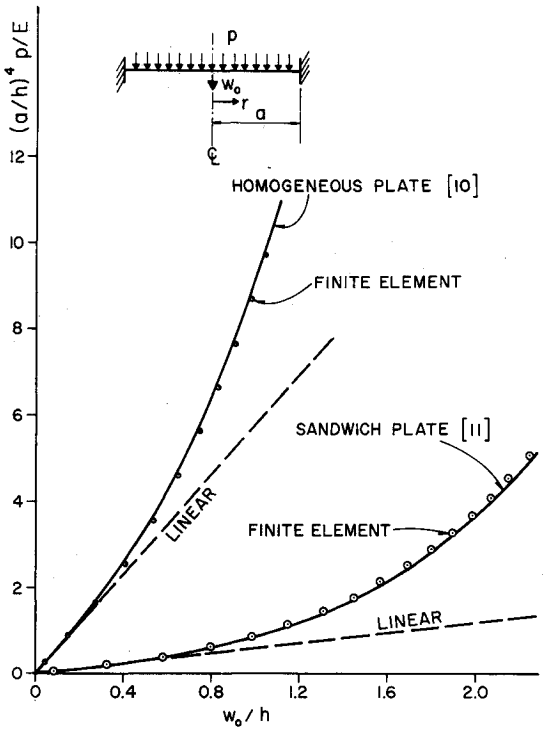

Fig. 4 Center deflections of the circular plates.

According to this method, the structure under consideration is augmented by providing a number of fictitious springs under the loaded degrees of freedom. The stiffness matrix of the augmented structure is then computed and used in Eqs. (24) to obtain the displacements of the actual structure. It has been shown[4] that the above stiffness matrix can be obtained by superposing the following matrix of rank one on the structural stiffness matrix K

$$[K_A] = (c/\sigma^2)\{R\}\{R\}^T \tag{25}$$

where c is the given stiffness of a fictitious elastic spring, $\{R\}$ is the structural load vector, and σ is the norm of vector $\{R\}$. Hence, the augmented equilibrium equations can be written as

$$[K+K_A]\{r\} = \{R\} \tag{26}$$

Note, that, substituting Eq. (25) into Eq. (26) yields

$$[K]\{r\} = \Lambda\{R\} \tag{27}$$

where Λ is a scalar load factor given by

$$\Lambda = 1-(c/\sigma^2)\{R\}^T\{r\} \tag{28}$$

which can be computed once Eqs. (26) are solved for $\{r\}$. If a proper choice for the value of c is made so that $[K+K_A]$ remains positive-definite throughout the range of analysis, $0 < \Lambda < 1$ on the ascending branch, and $-1 < \Lambda < 0$ on the descending branch of the load-deflection curve. For further discussion on this subject see Refs. 4 and 8.

Numerical Examples

Based on the foregoing formulation, a computer program was written for the solution of some numerical problems. The structures considered include circular plates and spherical caps with homogeneous and sandwich construction. The nonlinear bending and buckling problems of some of such structures were analyzed and the results are presented below.

1. Circular Plates

A clamped circular plate under a uniform lateral pressure, p, is considered with the following geometric characteristics: radius $a = 20$ in.; $h_f = 0.025$ in.; $h_c = 0.45$ in.; $h = 0.50$ in. The plate is divided into eight equally spaced elements, and the analysis is carried out for the following cases.

a) Sandwich construction having the following material properties: $E_f = E = 10^7$ psi; $G_c = 1500$ psi; $\nu_f = 0.25$. Furthermore, the core is assumed soft in the face parallel direction, and the shear deformations of the facings are neglected by assigning: $E_c = 0$; $G_f = 10^{15}$ psi.

b) Homogeneous construction with the following material properties: $E_f = E_c = E = 10^7$ psi; $\nu_f = \nu_c = 0.30$. To minimize the shear deformations, it is assumed that: $G_f = G_c = 10^{10}$ psi.

The results of these analyses are shown in Figs. 4 and 5 with circles. Figure 4 shows the normalized load-center deflection of the above plates. With the material properties assumed, these results can be compared with the nonlinear solutions of Way[10] for the homogeneous plate, and with that of Smith[11] for the sandwich plate. This comparison shows a close agreement between the present results and the above analytical solutions. It is of interest to note that the range of deflections for which the linear theory is applicable is of the order of one-half plate thickness for the homogeneous plate, and composite thickness for the sandwich plate.

The accuracy of the finite element analysis is further assessed in Fig. 5. In this figure, the variations of edge moment and in-plane force, in the radial direction, are shown as a function of applied pressure for the homogeneous plate. As shown, the agreement between the finite element results and the analytical solution of Ref. 10 is quite satisfactory. For the sandwich plate, the corresponding results are not shown, as no analytical solution was available.

The number of load increments used in obtaining the foregoing results was 44 for Sec. a and 21 for Sec. b. The computer time per element per load increment was 0.84 sec (cp).‡

2. Symmetrical Buckling of a Shallow Spherical Shell

Theoretical studies of the buckling problem of spherical caps have received considerable attention in the past decade. As a

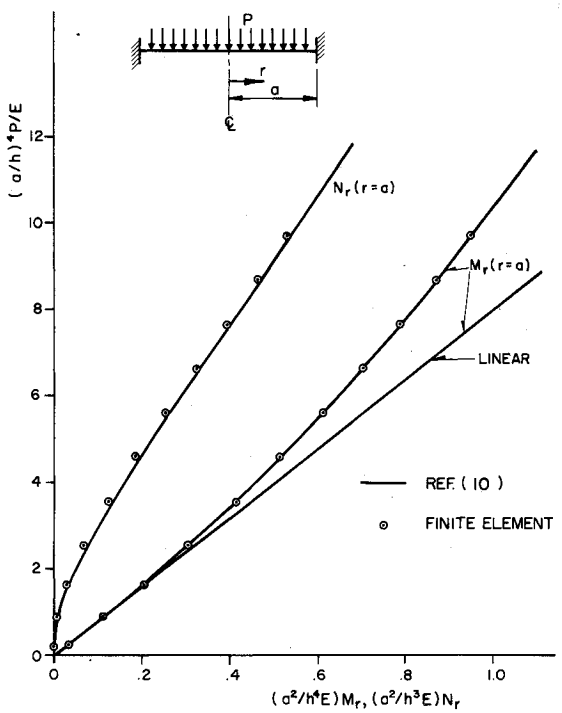

Fig. 5 Edge moment and in-plane force of the homogeneous circular plate.

‡ Central Processor, CDC 6400, University of California Computer Center, Berkeley, Calif.

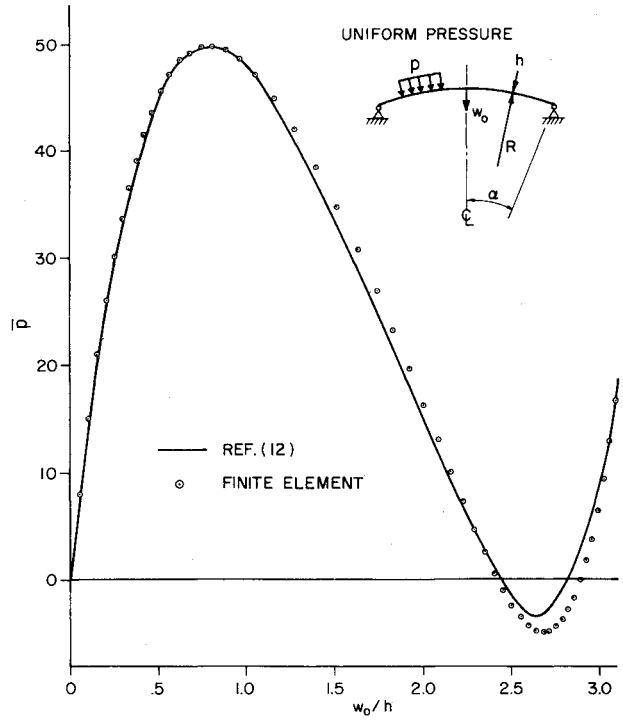

Fig. 6 Symmetrical buckling of a homogeneous cap.

result of these investigations, a geometric parameter has been devised to predict the buckling behavior of these structures. Weinitschke[12,13] has defined this parameter as $\mu^2 = m^2(R/h)\alpha^2$, where R is the radius of middle surface, α is the semiangle of shell opening, h is the thickness, and $m^2 = [12(1-\nu^2)]^{1/2}$, in which ν is the Poisson's ratio. In the case of homogeneous simply supported spherical shell under uniform lateral pressure, it has been shown that[13]: a) The buckling is associated with a symmetrical mode (snap-through phenomenon) when $2.2 \leqq \mu \leqq 4$; b) the buckling is associated with an asymmetrical mode (bifurcation phenomenon) when $\mu > 4$.

Asymmetrical buckling of axisymmetric shells cannot be investigated with the present formulation. Therefore, to show the application of the method to buckling and postbuckling problem of axisymmetrical shells, a spherical cap of type a is considered. It has the following characteristics: $h_f = 0.01$ in.; $h_c = 0.08$ in.; $h = 0.10$ in.; $R = 50$ in.; $\alpha = 4.48°$. In order to compare the results with the analytical solutions reported in Ref. 12, a homogeneous construction is assumed. Hence, for all layers: $E = 10^7$ psi; $G = 4 \times 10^6$ psi; and $\nu = 1/3$. Furthermore, the cap is simply supported and is under uniform lateral pressure p. For this cap $\mu^2 = 10$; therefore the shell should buckle symmetrically.

For the analysis of this shell, ten elements and 52 load increments were used. For postbuckling analysis, the structure was augmented using fictitious elastic spring of $c = 10{,}000$ lb/in.

The results of this analysis is shown in Fig. 6. The load parameter $\bar{p}$, in this figure, is defined as $\bar{p} = (\mu^2 m^2/4E)(R/h)^2 p$. Weinitschke, using a power series method, has solved this problem.[12] His result is also shown in the figure. The agreement between the two solutions, except at the lower critical load, is good.

The computer solution time for this problem was 0.9 sec (*cp*) per element per increment. This indicates less than 8% increase over the previous examples. The extra effort required by the augmentation process, accounts for this increase.

3. Elastic-Plastic Buckling of a Sandwich Cap

The sandwich cap shown in Fig. 7 is made of honeycomb core and identical aluminum face sheets. Its geometrical and material characteristics are: $h_f = 0.0076$ in., $h_c = 0.125$ in., $R = 19.68$ in., $a = 20.0$ in., $E_f = 10.35 \times 10^6$ psi, $G_f = 3.98 \times 10^6$ psi, $\nu_f = 0.3$, $E_c = 60{,}000$ psi, $G_c = 26{,}000$ psi, $\nu_c = 0.154$, and in the plastic range, $\sigma_y = 15{,}000$ psi and $E_t = 1.485 \times 10^6$ psi which are, respectively, the average yield stress and tangent modulus of the face sheets.

Using nine elements, the elastic (assuming fixed supports), and elastic-plastic (assuming both fixed and simple supports) buckling behavior of this cap was analyzed under a uniform external pressure p. The finite element results are shown in Fig. 7. Also shown are the Lin's[14] experimental buckling load and the predicted buckling loads using Yao's[15] linear eigenvalue solution. For the latter, two values are shown. The one designated as elastic is obtained using elastic moduli. The other predicted value is obtained using the following reduced modulus for the facings

$$E_r = 2E_t E_f/(E_t + E_f) = 2.6 \times 10^6 \text{ psi}$$

In Fig. 7 all the results are normalized with respect to Yao's reduced modulus solution of $P_{cr} = 33.5$ psi and the composite thickness of the cap, i.e., $h = h_c + 2h_f$. Comparing the finite element solutions with the above experimental and predicted buckling loads indicates a good correlation between the elastic-plastic finite element results and those of Lin's experimental and Yao's reduced modulus theory. Also, the locations of the buckles which according to finite element solutions occurred at the radial distances of 0.69a and 0.80a from the centerline (see Fig. 7) are in qualitative agreement with Lin's observation.[14]

Summary and Conclusions

An incremental displacement formulation has been presented for the nonlinear analysis of axisymmetric sandwich shells. Both geometric and material nonlinearities are considered. That is, large displacements, as a result of finite rotations, and plastic deformations of the facings are included in the present analysis. The sandwich construction considered has similar facings and isotropic material properties. Shear deformations, extensional, and flexural stiffnesses of all three layers are taken into account.

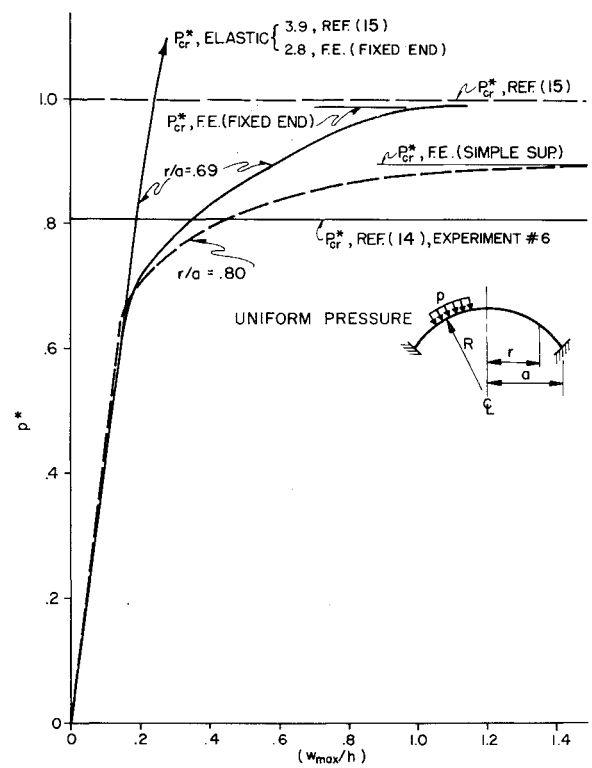

Fig. 7 Elastic-plastic buckling of a sandwich cap.

The discrete model is obtained using a doubly curved ring element. An incremental variational form, based on a moving reference configuration, has been used to derive the element equilibrium equations. These equations contain a load correction term which improves the accuracy and convergence. Incremental Lagrangian forms of stress-strain and strain-displacement relations, subject to the assumptions of finite rotations but infinitesimal strains, have been utilized in these derivations.

Perhaps the most significant aspect of the present nonlinear analysis is its capability to analyze buckling and postbuckling problems. For the latter, an augmentation scheme has been utilized which results in a positive definite stiffness matrix in the descending branch of the load-deflection curve. This technique proved to be quite effective in the solution of such problems. The extra computational effort required, it is felt, is outweighed by its usefulness.

Several numerical examples have been worked out to illustrate the applications of the method to nonlinear bending and buckling problems of axisymmetric plates and shells. In the elastic range, structures with both homogeneous and sandwich construction were analyzed; but in the plastic range, only sandwich shells with soft core and thin facings were considered. The results compare favorably with the analytical and experimental data available in the literature.

Appendix A: Strain-Displacement Relations for Axisymmetric Monocoque Shells

The nonlinear incremental strain-displacement relations including the effects of transverse shear deformations of an axisymmetric monocoque shell with axisymmetric deformations are derived subject to the following assumptions. 1) The shell is thin, i.e., the ratios of the thickness to the principal radii of curvature are small compared to unity. 2) The shell reference surface bisects the thickness. 3) In-plane strains and displacements vary linearly across the thickness. Transverse shear strains are constant across the thickness. 4) The normal strain in transverse direction is neglected. 5) The triple products of the linear components of strains, rotations, and their derivatives are negligible.

Following Novozhilov's approach,[16] the following axisymmetric displacement field is assumed:

$$u(\alpha_1,\zeta) = u^0(\alpha_1)+\zeta\beta(\alpha_1) \tag{A1a}$$

$$w(\alpha_1,\zeta) = w^0(\alpha_1)+\zeta\psi(\alpha_1) \tag{A1b}$$

where u and w are, respectively, the meridional and normal (radial) components of the incremental displacement vector of any point in the shell proper; u^0 and w^0 are the displacement components of a point in middle surface; ζ is a normal coordinate line with its origin in the middle surface; and β (rotation of the normal to the middle surface) and ψ are introduced to give a linear variation of displacements across the thickness. Note that assumption 4, which will be imposed later, is not satisfied by the Eq. (A1b).

The nonlinear strain-displacement relations are obtained using[16]

$$\varepsilon_{ij} = e_{ij}+\tfrac{1}{2}(e_{ki}-\omega_{ki})(e_{kj}-\omega_{kj}) \tag{A2}$$

where in the case of thin shells of revolution with the displacement field (A1).

$$\begin{aligned} e_{11} &= e_{11}{}^0+\zeta\left(\frac{\partial\beta}{\partial s}+\frac{\psi}{R_1}\right)\\ e_{22} &= e_{22}{}^0+\frac{\zeta}{r}(\beta\cos\phi+\psi\sin\phi)\\ e_{33} &= \psi,\quad e_{23} = e_{12} = 0\\ 2e_{13} &= 2e_{31} = (\beta-\chi)+\zeta[\partial\chi/\partial s-\beta/R_1] \end{aligned} \tag{A3a–e}$$

are the linear components of the strain tensors, and

$$2\omega_{31} = -2\omega_{13} = (\beta+\chi)-\zeta(\partial\psi/\partial s-\beta/R_1) \tag{A3f}$$

is the only nonzero rotation tensor.

Here

$$\begin{aligned} e_{11}{}^0 &= \partial u^0/\partial s+w^0/R_1\\ e_{22}{}^0 &= (1/r)(u^0\cos\phi+w^0\sin\phi) \end{aligned} \tag{A4a–b}$$

are the linear components of the middle surface strains in meridional and hoop directions, respectively

$$\chi = u^0/R_1-\partial w^0/\partial s \tag{A4c}$$

is the rotation of the tangent to the middle surface; $ds = R_1\,d\phi$; $r = R_2\sin\phi$; R_1 and R_2 are the principal radii of curvature; s and ϕ are, respectively, the arc length and the coordinate angle in the meridional direction.

By invoking assumption 4, Eqs. (A2) and (A3) yield $\varepsilon_{33} = \frac{1}{2}\beta^2+\psi(1+\psi/2) = 0$. Therefore

$$\psi = -\tfrac{1}{2}\beta^2/(1+\psi/2) \approx -\tfrac{1}{2}\beta^2 \tag{A5}$$

where $\psi/2$ is neglected in comparison to unity.

Substituting Eqs. (A3) and (A5) into (A2), and introducing assumptions 3 and 5 results in

$$\begin{aligned} \varepsilon_{11} &= e_{11}{}^0(1+\tfrac{1}{2}e_{11}{}^0)+\tfrac{1}{2}\chi^2+\zeta[(\partial\beta/\partial s)(1+e_{11}{}^0)+(\beta/R_1)(\chi-\tfrac{1}{2}\beta)]\\ \varepsilon_{22} &= e_{22}{}^0(1+\tfrac{1}{2}e_{22}{}^0)+(\zeta\beta/r)[\cos\phi(1+e_{22}{}^0)-(\beta/2)\sin\phi]\\ 2\varepsilon_{13} &= 2\varepsilon_{31} = \beta(1+e_{11}{}^0)-\chi,\quad \varepsilon_{33} = \varepsilon_{12} = \varepsilon_{23} = 0 \end{aligned} \tag{A6a–d}$$

which are the required nonlinear incremental strain-displacement relations.

Appendix B: Elastic-Plastic Constitutive Relations

Assuming infinitesimal deformations (strains), but finite rotations, the incremental strain, $\bar{\varepsilon}_{ij} = {}^2\varepsilon_{ij}-{}^1\varepsilon_{ij}$, can be decomposed into elastic, $\bar{\varepsilon}_{ij}{}^E$ and plastic, $\bar{\varepsilon}_{ij}{}^P$ components, i.e.

$$\bar{\varepsilon}_{ij} = \bar{\varepsilon}_{ij}{}^E+\bar{\varepsilon}_{ij}{}^P \tag{B1}$$

Note that in terms of three-dimensional Cartesian tensors

$${}^1\varepsilon_{ij} = \tfrac{1}{2}[(\partial z_m/\partial\bar{z}_i)(\partial z_m/\partial\bar{z}_j)-\delta_{ij}]$$

and

$${}^2\varepsilon_{ij} = \tfrac{1}{2}[(\partial Z_m/\partial\bar{z}_i)(\partial Z_m/\partial\bar{z}_j)-\delta_{ij}]$$

where $\bar{z}_i$, z_j and Z_i are, respectively, the Cartesian coordinates of a material point of a body in its undeformed and deformed configurations C_1 and C_2. Therefore, the relation between the incremental strain $\bar{\varepsilon}_{ij}$ and the one used in the text, $\varepsilon_{ij} = \frac{1}{2}[(\partial Z_m/\partial z_i)(\partial Z_m/\partial z_j)-\delta_{ij}]$, can be expressed as

$$\bar{\varepsilon}_{ij} = L_{ijmn}\varepsilon_{mn} \tag{B2a}$$

where

$$L_{ijmn} = (\partial z_i/\partial\bar{z}_m)(\partial z_j/\partial\bar{z}_n) \tag{B2b}$$

The elastic component, $\bar{\varepsilon}_{ij}{}^E$, is related to the incremental stresses through the elastic material law,[17] i.e.,

$$\bar{s}_{ij} = E_{ijmn}\bar{\varepsilon}_{mn} \tag{B3}$$

where E_{ijmn} is the rigidity tensor; $\bar{s}_{mn} = {}^2s_{mn}-{}^1\bar{s}_{mn}$ is the increment of the Piola stress tensor defined in terms of the unit area and coordinates of the undeformed configuration. The following relation holds between $\bar{s}_{ij}$ and the incremental stress tensor s_{ij} which is used in the text[4]:

$$s_{ij} = J^{-1}L_{ijmn}\bar{s}_{mn},\quad J = \det(\partial z_i/\partial\bar{z}_j) \tag{B4}$$

The plastic increment of strain is derived using von Mises yield function and its associated flow rule, i.e.,

$$F = [\tfrac{3}{2}{}^1t_{ij}{}^1t_{ij}]^{1/2}-k({}^1\varepsilon_{ij}{}^P) = 0 \tag{B5}$$

$$\bar{\varepsilon}_{ij}{}^P = \lambda\partial F/\partial{}^1\bar{s}_{ij} \tag{B6}$$

Here F is the yield function based on isotropic hardening law in which k is a measure of strain hardening and is a function of equivalent plastic strain, i.e.,

$${}^1\varepsilon_e{}^P = \int_0^{{}^1\varepsilon_{ij}{}^P} d\varepsilon_e{}^P,\quad d\varepsilon_e{}^P = [\tfrac{2}{3}d^1\varepsilon_{ij}{}^P\,d^1\varepsilon_{ij}{}^P]^{1/2} \tag{B7}$$

${}^1t_{ij} = {}^1\tau_{ij}-\frac{1}{3}\delta_{ij}{}^1\tau_{mm}$ is the Cauchy deviatoric stress tensor and λ is a nonzero scalar given by[4]

$$\lambda = -\frac{\hat{c}F}{\hat{c}^1\bar{s}_{mn}}\bar{s}_{mn}\Big/\frac{\hat{c}F}{\partial^1\bar{\varepsilon}_{kl}^P}\frac{\hat{c}F}{\partial^1\bar{s}_{kl}} \tag{B8}$$

where it is assumed that $\bar{s}_{mn} \simeq d^1 s_{mn}$.

Using Eq. (B5) and the relation ${}^1\tau_{ij} = J^{-1}L_{ijmn}{}^1\bar{s}_{mn}$, the above derivatives can be expressed as

$$\frac{\partial F}{\partial^1\bar{s}_{ij}} = \frac{3}{2\bar{\sigma}}P_{ijmn}{}^1\bar{s}_{mn} \tag{B9a}$$

$$\frac{\hat{c}F}{\hat{c}^1\bar{\varepsilon}_{ij}^P} = -\frac{\hat{c}k}{\hat{c}^1\bar{\varepsilon}_{ij}^P} = -\frac{H'}{\bar{\sigma}}{}^1\bar{s}_{ij} \tag{B9b}$$

where $\bar{\sigma} = [\frac{3}{2}{}^1t_{ij}{}^1t_{ij}]^{1/2}$ is the equivalent stress; $P_{ijmn} = J^{-2}(q_{im}q_{jn} - \frac{1}{3}q_{ij}q_{mn})$; $q_{ij} = 2{}^1\varepsilon_{ij} + \delta_{ij}$; $H' = \hat{c}\bar{\sigma}/\hat{c}^1\bar{\varepsilon}_e^P = E\rho/(1-\rho)$; $\rho = E_t/E$, and E and E_t are the elastic and tangent moduli, respectively.

Using Eqs. (B1, B3, and B6) together with Eqs. (B8) and (B9) the following elastic-plastic constitutive relation is obtained.

$$\bar{s}_{ij} = C_{ijmn}\bar{\varepsilon}_{mn} \tag{B10}$$

where

$$C_{ijmn} = E_{ijmn} - (1/h)B_{ijmn} \tag{B11a}$$

$$B_{ijmn} = 4\mu^2 f_{ij}f_{mn} + \lambda^2\theta^2\delta_{ij}\delta_{mn} + 2\mu\lambda\theta(f_{ij}\delta_{mn} + f_{mn}\delta_{ij}) \tag{B11b}$$

and

$$f_{ij} = (3/2\bar{\sigma})P_{ijmn}{}^1\bar{s}_{mn}, \quad \theta = f_{ii}$$
$$h = 2\mu f_{kl}f_{kl} + \lambda\theta^2 + (H'/\bar{\sigma})^1\bar{s}_{ij}f_{ij}, \quad \mu = E/[2(1+\nu)]$$
$$\lambda = 2\nu\mu/(1-2\nu)$$

and ν is the Poisson's ratio.

Using the relations (B2) and (B4), Eq. (B10) can be transformed in terms of the incremental stresses/strains used in this paper, i.e.,

$$s_{ij} = J^{-1}L_{ijmn}C_{mnkl}L_{klrt}\varepsilon_{rt} \tag{B12}$$

The above constitutive relations remain invariant in an orthogonal curvilinear coordinate system, provided that the Cartesian tensors are replaced by their respective physical components.

References

[1] Abel, J. F. and Popov, E. P., "Static and Dynamic Finite Element Analysis of Sandwich Structures," *Proceedings of the Second Conference on Matrix Methods in Structural Mechanics*, AFFDL-TR-68-150, 1968, pp. 213–245.

[2] Monforton, G. R. and Schmit, L. A., Jr., "Finite Element Analysis of Sandwich Plates and Cylindrical Shells with Laminated Faces," *Proceedings of the Second Conference on Matrix Methods in Structural Mechanics*, AFFDL-TR-68-150, 1968, pp. 573–608.

[3] Schmit, L. A., Jr. and Monforton, G. R., "Finite Deflection Discrete Element Analysis of Sandwich Plates and Cylindrical Shells with Laminated Faces," *AIAA Journal*, Vol. 8, No. 8, Aug. 1970, pp. 1454–1461.

[4] Sharifi, P., "Nonlinear Analysis of Sandwich Structures," Ph.D. dissertation, 1970, Structural Engineering and Structural Mechanics Dept., Univ. of California, Berkeley, Calif.

[5] Khojasteh-Bakht, M., "Analysis of Elastic-Plastic Shells of Revolution Under Axisymmetric Loading by the Finite Element Method," SESM 67-8, April 1967, Structural Engineering Lab, Univ. of California, Berkeley, Calif.

[6] Popov, E. P. and Sharifi, P., "A Refined Curved Element for Thin Shells of Revolution," *International Journal for Numerical Methods in Engineering*, Vol. 3, No. 4, 1971, pp. 495–508.

[7] Yaghmai, S. and Popov, E. P., "Incremental Analysis of Large Deformations in Continuum Mechanics with Applications in Elasticity," *International Journal of Solids and Structures*, Vol. 7, No. 10, 1971, pp. 1375–1393.

[8] Sharifi, P. and Popov, E. P., "Nonlinear Buckling Analysis of Sandwich Arches," *Journal of the Engineering Mechanics Division, ASCE*, Vol. 97, No. EM5, Oct. 1971, pp. 1397–1412.

[9] Whitman, E. and Gaylord, E. H., "Analysis of Unbraced Multistory Steel Rigid Frames," *Proceedings of the ASCE, Journal of the Structural Division*, Vol. 94, No. ST5, Aug. 1968, pp. 1143–1163.

[10] Way, S., "Bending of Circular Plates with Large Deflections," *Transactions of ASME*, Vol. 56, 1934, pp. 627–636.

[11] Smith, C. V., Jr., "Effect of Shear Deformation on Large Deflections of Circular Sandwich Plates," *AIAA Journal*, Vol. 6, No. 4, April 1968, pp. 721–723.

[12] Weinitschke, H., "On the Non-Linear Theory of Shallow Spherical Shells," *Journal of the Society for Industrial and Applied Mathematics*, Vol. 6, No. 3, Sept. 1958, pp. 209–232.

[13] Weinitschke, H., "On Axisymmetric Buckling of Shallow Spherical Shells," *Journal of Mathematics and Physics*, Vol. 44, No. 2, June 1965, pp. 141–163.

[14] Lin, M. S., "Buckling of Spherical Sandwich Shells," Ph.D. dissertation, 1968, Structural Engineering and Structural Mechanics Dept., Univ. of California, Berkeley, Calif.; also *Experimental Mechanics Journal*, Vol. 9, No. 10, Oct. 1969, pp. 433–440.

[15] Yao, J. C., "Buckling of Sandwich Sphere Under Normal Pressure," *Journal of the Aerospace Sciences*, Vol. 29, No. 3, Mar. 1962, pp. 264–268.

[16] Novozhilov, V. V., *Foundations of the Nonlinear Theory of Elasticity*, Graylock Press, Rochester, N.Y., 1953, pp. 186–193.

[17] Green, A. E. and Adkins, J. E., *Large Elastic Deformations*, Oxford University Press, London, 1960, pp. 4–6.